

Near-resonant effects in the quantum dynamics of the $\text{H}+\text{H}_2^+ \rightarrow \text{H}_2+\text{H}^+$ charge transfer reaction and isotopic variants

Cristina Sanz-Sanz,¹ Alfredo Aguado,¹ and Octavio Roncero^{2, a)}

¹⁾Unidad Asociada UAM-CSIC, Departamento de Química Física Aplicada, Facultad de Ciencias M-14, Universidad Autónoma de Madrid, 28049, Madrid, Spain

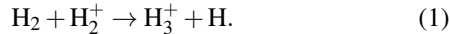
²⁾Instituto de Física Fundamental (IFF-CSIC), C.S.I.C., Serrano 123, 28006 Madrid, Spain

The non-adiabatic quantum dynamics of the $\text{H}+\text{H}_2^+ \rightarrow \text{H}_2+\text{H}^+$ charge transfer reactions, and some isotopic variants, is studied with an accurate wave packet method. A recently developed 3×3 diabatic potential model is used, which is based on very accurate *ab initio* calculations and includes the long-range interactions for ground and excited states. It is found that for initial $\text{H}_2^+(v=0)$, the quasi-degenerate $\text{H}_2(v'=4)$ non-reactive charge transfer product is enhanced, producing an increase of the reaction probability and cross section. It becomes the dominant channel from collision energies above 0.2 eV, producing a ratio, between $v'=4$ and the rest of v 's, that increases up to 1 eV. $\text{H}+\text{H}_2^+ \rightarrow \text{H}_2^++\text{H}$ exchange reaction channel is nearly negligible, while the reactive and non-reactive charge transfer reaction channels are of the same order, except that corresponding to $\text{H}_2(v'=4)$, and the two charge transfer processes compete below 0.2 eV. This enhancement is expected to play an important vibrational and isotopic effect that need to be evaluated. For the three proton case, the problem of the permutation symmetry is discussed when using reactant Jacobi coordinates.

Accepted in J. Chem. Phys. (2021),

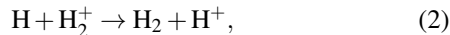
I. INTRODUCTION

Hydrogen is the most abundant element in Universe, with nearly 73% of the baryonic mass, and plays a fundamental role in the chemistry of the interstellar medium (ISM). It is at the origin of the chemical cycles of most of the molecules, which in turn play a fundamental role in the collapse of molecular clouds to form stars and planetary systems. The most abundant molecular species are H_2 and H_3^+ , while H_2^+ , formed by ionization of H_2 by cosmic rays, is rapidly destroyed by the exothermic reaction



H_3^+ is considered as the universal protonator^{1,2} by producing hydrides when colliding with atoms and molecules³⁻⁸. Its collisions with H_2 produce ortho/para transitions of the two species, and/or to its deuteration when colliding with HD isotopic variant.

In local galaxies, the formation of H_2 is attributed to reactions on cosmic grains and ices^{9,10}, because the gas phase routes have too low rate constants to reproduce the observed abundances. In Early Universe, where grains and ices do not exist, one of the key problems is therefore to determine the processes, and their related rate constants, giving rise to H_2 . One of this is the charge transfer reaction



where the reactant and product channels of Eq. 2 correspond to the first excited and the ground electronic states of the H_3^+ system, respectively.

H_3^+ plays a fundamental role in astrochemistry and it has been the subject of many studies summarized in

reviews^{1,2,7,11-13} and special issues^{14,15}. Its infrared spectrum was first detected in the laboratory by Oka¹⁶ and later in the space^{2,17-19}. Since then, H_3^+ has become commonly used to probe spacial conditions, such as a thermometer and a clock of cold molecular clouds²⁰. Its infrared spectrum has been theoretically characterized with spectroscopic accuracy²¹⁻²⁵, based on highly accurate potential energy surfaces (PESs), local²⁶⁻²⁸ and global^{22,29-35}.

The H^++H_2 exchange reaction has been the subject of many experimental³⁶⁻⁴⁵ and theoretical^{41,46-62} studies. This reaction governs the ortho/para transitions of H_2 and is also responsible of the H_2 deuteration. For energies below ≈ 1.82 eV, this reaction takes place in the ground singlet state of H_3^+ . In the ground H_3^+ electronic state there is a deep insertion well, of ≈ 4.6 eV, and the dynamics is mediated by a dense manifold of resonances, and exact calculations show that the reaction proceeds through a statistical mechanism⁵⁷⁻⁵⁹. Above 1.82 eV collision energy, the H_2^++H channel becomes accessible, opening the charge transfer process, inverse to the reaction 2, and has been studied in a broad energy range^{40,41,45-56,61,62}. Furthermore, the non-adiabatic transitions in H_3^+ were studied recently in photodissociation experiments by Urbain *et al.*⁶³.

In spite of all these studies on H_3^+ , reaction 2 has only been studied experimentally by Karpas *et al.*⁶⁴, by McCartney *et al.*⁶⁵, at energies of 30-100 keV, and more recently Andrianarijaona *et al.*^{66,67} studied the $\text{H} + \text{D}_2^+$ isotopic variant in a broader energy range of 0.1-100 eV. The experimental study of reaction 2 have the difficulty of involving two radical reactants, and accurate theoretical simulations are then of high interest to provide realistic rate constants for the model of Early Universe^{9,40,68-70}. Some approximated theoretical treatments where applied to reaction 2^{48,54,55,71,72}. Also, an accurate quantum treatment of this reaction was done very recently⁷³, during the publication of this work. In this work we present accurate quantum wave packet calculations of the $\text{H}+\text{H}_2^+$ charge transfer (CT) reaction, and some isotopic vari-

^{a)}Electronic mail: octavio.roncero@csic.es

ants, at collision energies below 1 eV using a very accurate set of three coupled PESs recently proposed⁷⁴, which include long range interactions for the ground and excited electronic states. The manuscript is distributed as follows. First, in section 2, a brief description of the PESs and dynamical methods are shown, presenting a description of the permutation symmetry problem. In section 3 the theoretical simulations are shown and discussed, and, finally, section 4 is devoted to extract some conclusions, outlining future work.

II. METHODOLOGY

A. Diabatic electronic representation

The potential used is described by a 3×3 diabatic matrix, each diagonal element corresponding to a positive charge in each of the nuclei⁷⁴. It consists of a zero-order diatomics-in-molecules (DIM) matrix⁷⁵, describing accurately the H_2 and H_2^+ diatomic fragments (shown in Fig. 1), plus three-body terms added in the diagonal, and non-diagonal matrix, V^{3B} , as it was proposed by Varandas and co-workers³⁴. In this potential the long range term has been improved⁷⁴ and included in all the electronic states. The dominant long range terms for $H+H_2^+$ are the charge-induced dipole and charge-induced quadrupole dispersion interactions, varying as R^{-4} and R^{-6} , respectively. For $H^+ + H_2$ the dominant long range terms are the charge-quadrupole and the charge-induced dipole dispersion energies, varying as R^{-3} and R^{-4} , respectively. The V^{3B} was fitted to very accurate *ab initio* calculations using multi-reference configuration interaction (MRCI) calculations, performed with the MOLPRO suite of programs⁷⁶. A complete basis set (CBS) approximation was done based on the aV5Z and aV6Z basis sets of Dunning⁷⁷. These V^{3B} matrix elements change gradually what allows a very accurate fitting, with a small root mean square error⁷⁴, what is an advantage as compared to the fitting of the sharply varying non-adiabatic matrix elements (NACMEs) required when using an adiabatic representation³⁵.

Diabatic representations are generally considered to be approximate, due to the impossibility to eliminate all NACMEs as a function of all internal coordinates because of the curl condition^{78,79}. The quasi-diabatic representation of the PES used here⁷⁴ is considered as a regularization representation^{80,81}, in which the singularities present at conical intersections (CI) are removed exactly⁸¹. In the vicinity of CIs the calculation of NACMEs presents numerical problems what adds some error in the adiabatic representation since the Born-Oppenheimer is ill-conditioned at CIs⁸². The resulting NACMEs obtained by Aguado *et al.*⁷⁴ showed to be in excellent agreement with the *ab initio* points. Moreover, the residual NACMEs appearing in all diabatic representation are very small in the present case, because the three-fold basis is rather complete in this system. These residual NACMEs are very small, and only appreciable far from CIs, where the energy difference among the different electronic states is so large that they can be neglected without loss of accuracy.

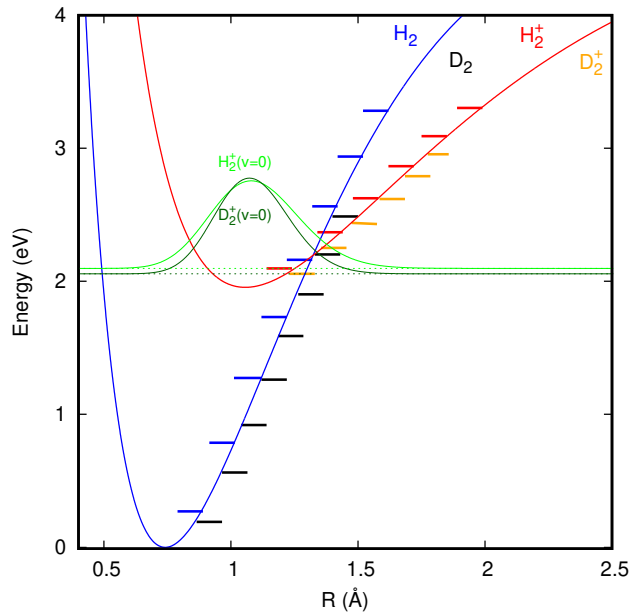


FIG. 1. Potential energy curves and vibrational levels of H_2 (D_2) and H_2^+ (D_2^+). The radial part of the nuclear wave functions for H_2^+ (D_2^+) have been represented in green.

Quasi-diabatic representations are not unique. In Ref.⁷⁴ it was considered a minimum basis set formed by 3 functions, denoted ϕ_i , in which there is a positive charge of nucleus i , and one $1s$ electron in the remaining nuclei. In this basis set, the excited $H_2^+(^2\Sigma_g^+)$ is a linear combination of at least two ϕ_i functions. A unitary transformation is done, in order to define properly the $H_2(^1\Sigma_g^+)$ and $H_2^+(^2\Sigma_g^+, ^2\Sigma_u^+)$ for a particular (reactant) rearrangement channel, as

$$\begin{aligned}\phi_1^1 &= \phi_1 \\ \phi_2^1 &= \frac{1}{\sqrt{2}}(\phi_2 - \phi_3) \\ \phi_3^1 &= \frac{1}{\sqrt{2}}(\phi_2 + \phi_3).\end{aligned}\quad (3)$$

Transforming the 3×3 potential accordingly, the H_2 and H_2^+ ground electronic states become diagonal in channel 1, corresponding to the hydrogen 1 at very long distances from the other two, and the corresponding potentials are shown in Fig. 1. However, on the other two rearrangements, the potential matrix is non diagonal, and the diabatic couplings are non-zero as can be seen in the right panels of Fig. 2, where they are represented in Jacobi coordinates, r and R for a collinear configuration. As a consequence, the rovibrational states of the products are expanded in several electronic states, for H_2 and H_2^+ as

$$\begin{aligned}\phi_{v'j'}^{i=2,3}(r') &= \sum_k \phi_k^1 C_k^{v'j'}(r') \\ \phi_{v'j'}^{i=2,3+}(r') &= \sum_k \phi_k^1 C_k^{v'j'+}(r'),\end{aligned}\quad (4)$$

respectively, where r' denotes the internuclear distance in the corresponding product Jacobi coordinates $r' = r_{13}$ or $r' = r_{12}$ for $i = 2$ and 3, respectively.

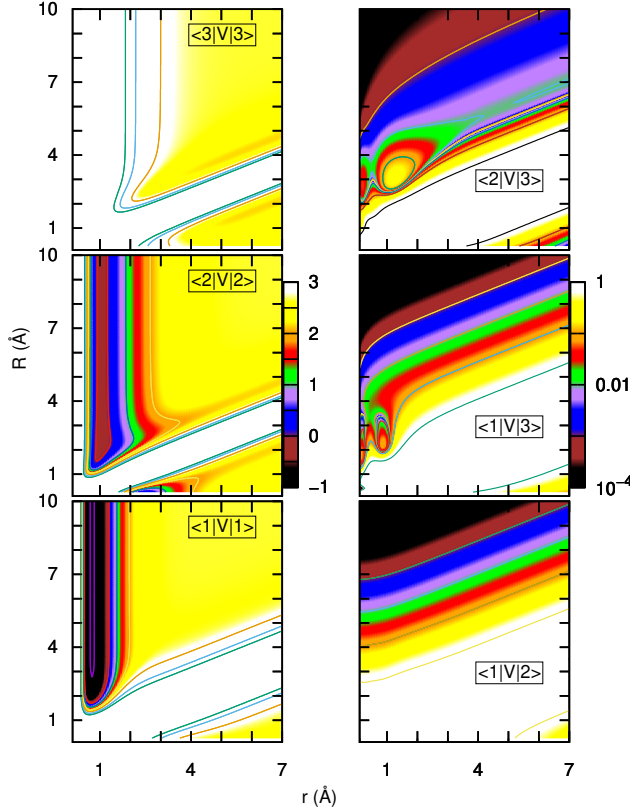
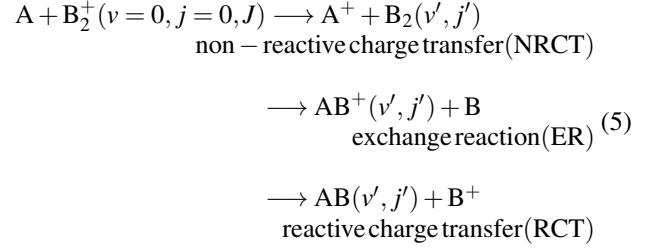


FIG. 2. Contour plots of the diagonal (left panels) and non-diagonal (right panels) elements of the 3×3 potential matrix at a Jacobi angle of 0° , as a function of the Jacobi distances r and R , in the diabatic representation of functions ϕ_i^1 . In the diagonal terms, the zero of energy is set at the eigen value of $\text{H}_2^+(v=0, j=0)$ ground rovibrational state, which is at 2.09 eV in Fig. 1. The absolute value of nondiagonal terms are plotted in logarithmic scale.

The diagonal and non-diagonal elements of the potential matrix in this diabatic representation are shown in Fig. 2 for a collinear configuration. For long R and short r values, the diagonal terms represent $\text{H}_2(1\Sigma_g^+)$ (bottom left panel), the $\text{H}_2(2\Sigma_g^+)$ (middle left panel) and $\text{H}_2(2\Sigma_u^+)$ (top left panel), the last being purely repulsive. The diagonal terms at long r and R values are repulsive, and do not represent the products channels because the non-diagonal terms (shown in the right panels) are non-zero and pretty large. In the reactant channels (long R and short r values) the $\langle 1|V|2 \rangle$ non-diagonal coupling term, coupling $\text{H}_2(2\Sigma_g^+)$ with $\text{H}_2(1\Sigma_g^+)$, decrease slowly with increasing R , being of the order of ≈ 1 meV at $R=7$ Å. This clearly shows that this charge transfer coupling extends towards very long R distances.

B. Quantum wave packet calculations

The reaction dynamics of the H/D collisions with $\text{H}_2^+(v=0, j=0)$ and H with $\text{D}_2^+(v=0, j=0)$ are studied here using a quantum wave packet method as implemented in the MADWAVE3 program^{57,83–86}. For each total angular momentum, J , the state-to-state S-matrix elements are calculated using a reactant Jacobi coordinate based method⁸⁷, generalized to consider product rovibrational states expanded in several electronic states, as in Eq. 4. Three different processes (α channels) are distinguished



with $A = \text{H}, \text{D}$ and $\text{B}_2 = \text{H}_2, \text{D}_2$. Channels $\alpha = 1$ (NRCT) and 3 (RCT) correspond to products in the ground adiabatic states, either in the reactants or products channels, respectively. Channel $\alpha = 2$ (ER) corresponds to exchange products in the first excited adiabatic state.

TABLE I. Parameters used in the wave packet calculations in reactant Jacobi coordinates: $r_{min} \leq r \leq r_{max}$ is the H_2 internuclear distance, $R_{min} \leq R \leq R_{max}$ is the distance between H_2 center-of-mass and the A atom, $0 \leq \gamma \leq \pi$ is the angle between \vec{r} and \vec{R} vectors.

$r_{min}, r_{max} = 0.1, 20$ Å	$N_r = 360$
$r_{abs} = 16$ Å	$\alpha_r = 10^{-3}, n=6$
$R_{min}, R_{max} = 0.01, 20$ Å	$N_R = 360$
$R_{abs} = 16$ Å	$\alpha_R = 10^{-3}, n=6$
$N_\gamma = 100$	in $[0, \pi/2]$
$R_0 = 14$ Å	$E_0, \Delta E = 0.5, 0.5$ eV
$R_\infty = 16$ Å	$R'_\infty = 10$ Å

The parameters used in the wave-packet calculations are listed in table I. Briefly, the initial wave packet corresponds to the product of the $\text{H}_2^+(v=0, j=0)$ ro-vibrational eigenfunction, a normalized Wigner function for J and a real Gaussian function, describing the translation on the R Jacobi distance (between the incoming A atom and the center of mass of H_2^+), initially placed at R_0 , with a central energy E_0 and an energy width ΔE . The flux on individual rovibrational states are analysed at R_∞ and R'_∞ for reactants and products, respectively. The wave packet is absorbed at the edges of the radial grid by multiplying it by an absorbing function $e^{\alpha_\rho(\rho - \rho_{abs})^n}$ for $\rho \geq \rho_{abs}$ ($\rho = r$ or R) at each Chebyshev iteration, using a modified Chebyshev propagator⁸⁸. Using this propagator only a real wave packet is propagated^{57,89–91}, and the corresponding kinetic term is evaluated using a sine Fourier transform which ensures the proper regular behaviour at $R = 0$ ⁹², appearing in this reaction. Finally, a Gauss-Legendre quadrature is used to describe the Jacobi angle $\cos \gamma = \mathbf{r} \cdot \mathbf{R} / rR$, and

the corresponding kinetic terms are evaluated using a Discrete Variable Representation (DVR) method⁹³. For $J=0$, about 8×10^4 iterations are needed to converge the reactions probability down to 0.01 eV. This long propagation is needed because of the presence of resonant structures that will be commented below. This is also the situation of higher J until the rotational barrier push the reactive and NRCT probabilities towards higher energy, what happens at $J=14$ and 17 for $H/D + H_2^+$ cases, respectively. For higher J 's, the number of iterations needed gradually decreases.

The calculations have been performed for all J up to $J=15$ and $J=20$ for $A=H$ and D , respectively. For higher values of J , wave packet calculations are performed every 5 J values up to $J=60$ and $J=80$, for $A=H/D$, respectively. A maximum of helicity components $\Omega_{max} = 23$ is considered in the $J > 0$ calculations. For intermediate J values, where no wave packet calculations were done, an interpolation method based⁹⁴ on the J -shifting⁹⁵ approximation is performed to evaluate the individual state-to-state S^2 matrix elements⁹⁴.

The state-to-state integral cross sections are then evaluated using the usual partial wave expansion as

$$\sigma_{\alpha v_j \rightarrow \alpha' v' j'}(E) = \frac{\pi k_{\alpha v_j}^{-2}}{(2j+1)} \sum_{J, \Omega} (2J+1) \left| S_{\alpha v_j \Omega \rightarrow \alpha' v' j' \Omega}^J(E) \right|^2 \quad (6)$$

C. Symmetry considerations

Dealing with two ($D+H_2^+$) or three ($H+H_2^+$) hydrogen atoms, fermions with nuclear spin $i=1/2$, some considerations about the permutation symmetry should be done. The total wave function has to be antisymmetric under the exchange of any hydrogen pair. The total wave function can be factorized as a product of electronic, nuclear spin and rovibrational components as $\Psi = \Psi_e \Psi_I \Psi_{Rot}$. The symmetry of the electronic function, Ψ_e , is analyzed in the body fixed frame of the nuclei, and the permutation of any pair of nuclei corresponds to a reflection through a plane perpendicular to the molecular plane⁹⁶. In this case, all singlet states of H_3^+ are totally symmetric. The nuclear spin functions, Ψ_I , are characterized by the total nuclear spin, I_2 and I_3 , for 2 and 3 hydrogen systems, respectively. $I_2 = 0$ and 1 , and the corresponding functions Ψ_{I_2} are antisymmetric and symmetric with respect to the permutation of the two hydrogen atoms, respectively. To make the total wave function antisymmetric, the corresponding rovibrational function have to be symmetric and antisymmetric for $I_2 = 0$ and 1 , respectively. In diatomic molecules, this corresponds to the usual separation between even and odd rotational levels, since the symmetry of spherical harmonic is $(-1)^j$, denoted as para and ortho, respectively.

For three hydrogen atoms system, $I_3 = 1/2$ and $3/2$, and the spin functions can be written as $|I_3 M_3; i_2\rangle = \sum_{\sigma m_2} \langle i_2, 1/2 | m_2, \sigma, I_3 M_3 | 1/2, \sigma \rangle |i_2, m_2\rangle$, where $|i_2, m_2\rangle$ is the spin function of two hydrogen, each one described by $|1/2, \sigma\rangle$, and $\langle \rangle$ are Clebsch-Gordan coefficients. The existing functions are then $|3/2 M_3; 1\rangle$, $|1/2 M_3; 1\rangle$ and $|1/2 M_3; 0\rangle$, with $I_3 = 3/2$, $1/2$ and $1/2$, respectively. Considering the D_{3h}

permutation-inversion group, the spin functions with $I_3=3/2$ (ortho) belong to the A_1 representation, while with $I_3 = 1/2$ (para) belong to the E representation. To build antisymmetric total wave functions, the corresponding rovibrational components have to belong to A_2 (for $I_3=3/2$, ortho) and E (for $I_3=1/2$, para) representations. It should be noted here, that the product for $I_3=1/2$, the total symmetry is $E \times E = A_1 + A_2 + E$, and only A_2 is anti-symmetric while the other solutions are not physically allowed.

All this said, and neglecting the weak hyperfine nuclear spin rotation coupling, the spin of each hydrogen atom is conserved, and therefore the transformation from ortho to para, and viceversa, can only take place by hydrogen exchange, *i.e.*, by a reaction.

When using reactant Jacobi coordinates, the permutation symmetry of the $D+H_2^+$ and $H + D_2^+$ is fully account for, while this is not the case for $H+H_2^+$. In the three identical hydrogen atoms case, the A_2 and E representation has to be considered, separately, while the A_1 does not exist. Thus, the diatomic rotational channels (for reactants and products) included in each representation of the nuclear wave function are^{97,98}

$$\begin{aligned} E &: \text{even and odd } j, j' \rightarrow I_3=1/2, I_2=1, 0 \text{ (para) of } A_1 \\ A_1 &: \text{only even } j, j' \rightarrow \text{does not exist for } i=1/2 \\ A_2 &: \text{only odd } j, j' \rightarrow I_3=3/2 \text{ (ortho) of } A_1. \end{aligned}$$

Clearly the case of three identical hydrogens, with reactants in $j=0$, contains the E and A_1 representation of the D_{3h} inversion-permutation group. For the final reactants or products in even j' also contains E and A_1 representations and are therefore difficult to distinguish when using Jacobi coordinates. Finally, the initial case $j=0$ and final odd j' (para-to-ortho transition of dihydrogen molecules/cations) clearly belong to the E representation of H_3^+ .

Therefore, when using reactant Jacobi coordinates, total integral reaction cross sections can not be obtained, while the para-ortho state-to-state integral cross section can be obtained. However, when referring to $H+H_2^+$ ($v=0, j=0$) reaction dynamics we shall include all the cases, physical (E) and non-physical (A_1), to compare with the $D+H_2^+$ ($v=0, j=0$).

III. RESULTS

The reaction probabilities obtained for the three reactions under study for $J=0$ are shown in Fig. 3, separated for the three different processes of Eq. 5 and summing over all rotational states of products. The reactions for $H+H_2^+$ (left panels), $D+H_2^+$ (middle panels) and $H+D_2^+$ (right panels) show similar patterns, and each mechanism is discussed separately below.

For the three reactions, the NRCT process (in the top panels of Fig. 3) is open from zero collision energy. As displayed in Fig. 1, the H_2^+ ($v=0$) classical turning points appear at shorter distances than the crossing point between the H_2^+ and H_2 potential curves. However, the vibrational ground state of H_2^+ ($v=0$) and D_2^+ ($v=0$) have significant amplitude at the region of the crossing, see Fig. 1. This situation allows the electronic charge transfer in the same channel for long R distances, because the electronic coupling becomes effective (see

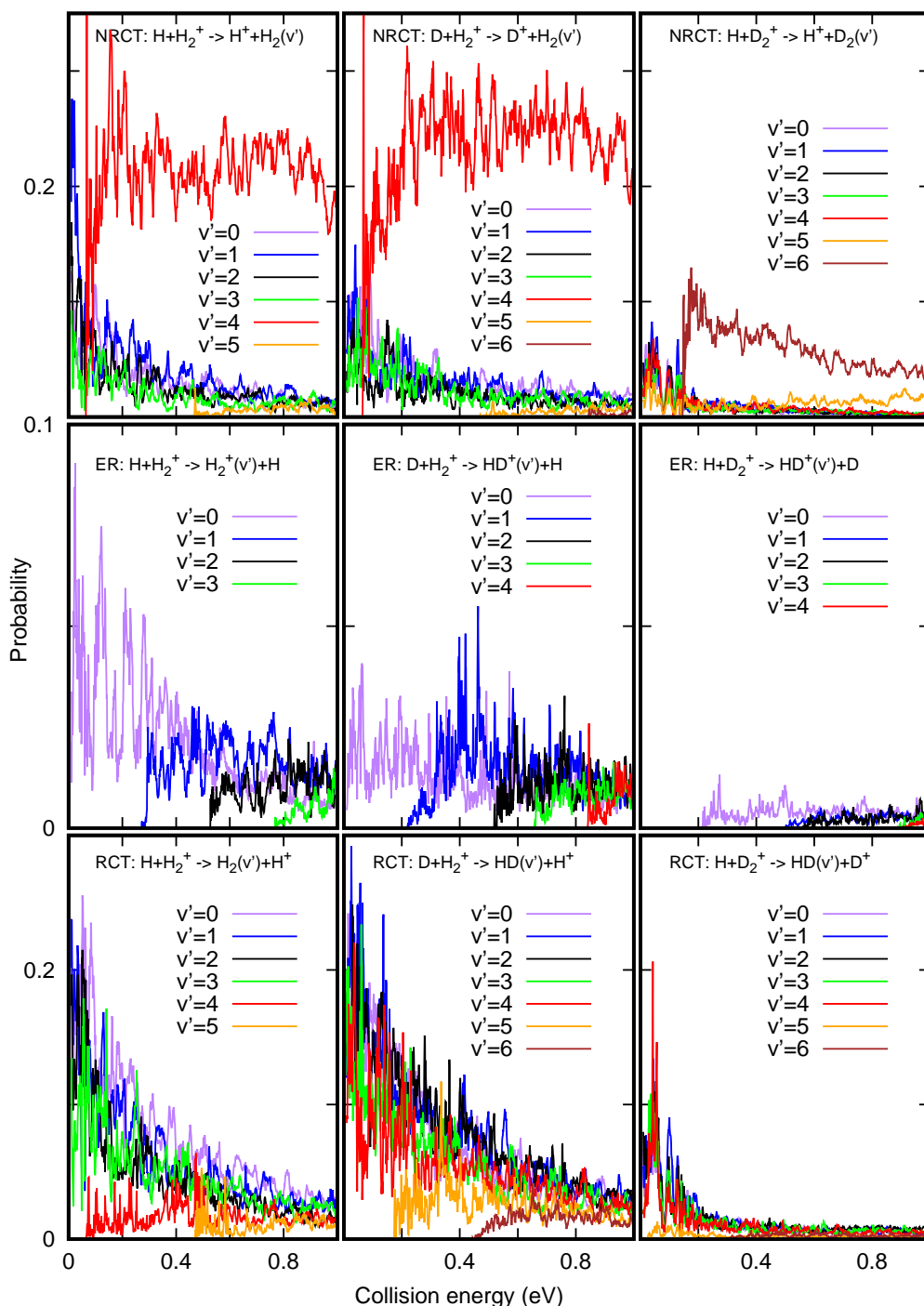


FIG. 3. Vibrationally resolved reaction probability for $\text{H}+\text{H}_2^+(v=0, j=0)$ (left panels), $\text{D}+\text{H}_2^+(v=0, j=0)$ (middle panels), and $\text{H}+\text{D}_2^+(v=0)$ (right panels), towards the inelastic charge transfer, NRCT (H^++H_2 , D^++H_2 and H^++D_2 , in the top panels), the exchange reactive channel, ER ($\text{H}+\text{H}_2^+$, $\text{H}+\text{HD}^+$ and $\text{D}+\text{HD}^+$, in the middle panels) and reactive charge transfer, RCT, channels (H^++H_2 , H^++HD and D^++HD , in the bottom panels).

Fig. 2).

This is particularly evident for $\text{H}_2(v'=4)$ which is nearly resonant with $\text{H}_2^+(v=0)$ (just 0.064 eV above), presenting a large vibrational overlap, what yields to a strong electronic transition to $\text{H}_2(v'=4)$. The ratio between the final probability in $\text{H}_2(v'=4)$ and all other channels increases with collision

energy. This clearly explains the experimental results⁶⁴, who found that charge transfer is the dominant mechanism, rather than hydrogen exchange or complex formation with scrambling. These two mechanisms, associated to ER and RCT, can compete at the lower energies considered here, as discussed below.

For $D_2^+(v=0)$, however, the energy differences with $D_2(v'=5,6)$ are larger, of ≈ 0.15 eV, and the amplitude of the $D_2^+(v=0)$ at the electronic crossing is lower (see Fig. 1). All these make less effective the electronic coupling. As a consequence, all the final vibrational channels have lower probability. In spite of the larger energy spacing, the $D_2(v'=6)$ level shows to be considerably more populated than any other vibrational level of D_2 , in clear analogy with the situation of H_2 .

The exchange reaction mechanism, ER in the middle panels of Fig. 3, are also non zero, even when it is less probable than the other two charge transfer mechanisms. The adiabatic potential for the first excited electronic state presents a rather high reaction barrier for the exchange. Therefore, ER proceeds in a two step mechanism. First, there is a transition to the ground electronic state, with a deep well, explaining the resonance structure present in the ER probabilities. This is followed by a second transition back to the excited $H + H_2^+/H+DH^+/D+DH^+$ channel, in each case respectively, giving rise to non-zero ER probabilities, lower than the RCT probabilities because there is a lower density of final states for H_2^+/HD^+ channels. The probability for the ER channel presents a clear decrease when the mass of reactants increase, from $H+H_2^+$, to $D+H_2^+$ and $H + D_2^+$.

The RCT mechanism (see bottom panels of Fig. 3) consists of two steps, a transition to the ground electronic state and the reactive exchange of a hydrogen atom. Except for $H_2(v'=4)$ (or $D_2(v'=6)$), the RCT probabilities are very similar to those of the NRCT channel. This could be explained by the near statistical mechanism of the reaction in the ground adiabatic state^{43,57,58,98}, that is, the reaction is mediated by resonances originated by the deep insertion well of the ground electronic state of H_3^+ . At collision energies below 1 eV these resonances are long lived and the reaction cross section and the final distribution of products are well described by statistical methods^{58,98}. At the higher energies considered here (about 1.8 eV above the ground H^++H_2 threshold), the resonance persist and a pseudo-statistical behaviour may be expected. This explains the resonance structure of all reaction probabilities in Fig. 3.

Three main differences are found with the previous results recently reported by Ghosh *et al.*⁷³. First, the results of Ref.⁷³ do not show the dense manifold of narrow resonances shown here. Also their probabilities do not show a progressive increase with decreasing collision energy, as the present ones do, associated to the long range interactions. Finally, the results of Ghosh *et al.*⁷³ do show a much lower increase of the NRCT for $H_2(v'=4)$, and instead their probabilities for $H_2(v'=3)$ are of the same order of $v'=4$. All these differences are attributed to the use of different PESs, and, in particular, to the electronic couplings producing the charge transfer. It is worth noting here, the coupling at relatively long distance plays an important role in the nearly resonant enhancement of the CT for $H_2(v'=4)$ obtained here. On the contrary, Ghosh *et al.*⁷³ used a relatively short initial distance of ≈ 5.6 Å as compared to $R_0=14$ Å used here.

The total reaction probabilities for each of the mechanisms and different values of total angular momentum, J , are shown

in Fig. 4 for $H+H_2^+, D+H_2^+$ and $H+D_2^+$ reactions. All the probabilities shift towards higher energies with increasing J . However, there are important differences. First, $D+H_2^+$ shows smaller shifts, simply because the effective rotational barrier decreases, because the reduced mass is larger, $\mu \approx 1, 4/5$ and $2/3$ amu for $D+H_2^+, H+D_2^+$ and $H+H_2^+$, respectively. The NRCT channel also shows a smaller shift with J , what is attributed to the long-range character of the electronic couplings, as described above. Moreover, this also explains why the NRCT probabilities increase near the rotational threshold while for ER and RCT the probabilities clearly decrease with J at the threshold. As the rotational barrier increases, it closes the access to reaction, while the NCR process is still possible due to long range non-adiabatic couplings, which are effective because the quasi-degeneracy of the $H_2^+(v=0)$ and $H_2(v'=4)$ levels, or equivalently $D_2^+(v=0)$ and $D_2(v'=6)$. This behavior also produces an enhancement of the NRCT mechanism as compared to ER and RCT channels, except for low collisions, where RCT mechanism dominates.

The opacity function, *i.e.* the reaction probabilities versus J , reported by Ghosh *et al.*⁷³ shows a sudden drop between 0.3 and 0.4 eV at $J=12$. However, in the present results the rotational threshold at 0.3 eV is approximately at $J=40$. A continuous and gradual increase of the rotational threshold is found here at all collision energies of Fig. 4. This difference with previous results⁷³ is attributed to the long-range behaviour of the electronic couplings and the longer distances considered in the dynamical calculations, as discussed above.

The total integral cross section for each of the processes are shown in Fig. 5 for the $H+H_2^+(v=0, j=0)$ (bottom panel), $D+H_2^+(v=0, j=0)$ (middle panel) and $H+D_2^+(v=0, j=0)$ (top panel) collisions. At 1 eV, $\sigma^{NRCT} > \sigma^{RCT} > \sigma^{ER}$, but the ratio changes with collision energy. The exchange reaction, ER, is always lower, since it involves 2 electronic transitions and the H_2^+/HD^+ products have a lower density as compared to H_2/HD . The NRCT/ER ratio is nearly constant with collision energy. On the contrary NRCT/RCT varies considerably, being nearly 1 for collision energies near 0.2 eV, and increases to 10/4/9 at 1.eV, for $H+H_2^+/D+H_2^+/H+D_2^+$ respectively. This ratio seems to increase with energy, in agreement with the experiments performed by Karpas *et al.*⁶⁴, who found that the CT dominates the $H+H_2^+$ reaction.

At low collision energies, before the dominant NRCT resonant $H_2(v'=4)$ or $D_2(v'=6)$ channel opens, RCT and NRCT cross sections are of the same order, and in most cases the RCT process dominates. In this region the dynamics is dominated by a statistical process: After a first electronic transition, the system gets trapped in the long-lived resonances originated by the deep H_3^+ well of the ground electronic state. At these long-lived resonances, energy transfer among all internal degrees of freedom becomes very effective and the products are formed proportionally with the density of states. Thus for H_2^+ , with three identical $H^+ + H_2$ charge transfer products, the NRCT/RCT reaches a factor between 0.5 and 1. For $D^+ + H_2$, this factor decreases, since HD^+ RCT products have larger density of states than $H_2^+ + D$. Finally, for $H+D_2^+$ the ratio of the density of products states is reversed becoming denser for the inelastic D_2 channel than for the reactive HD

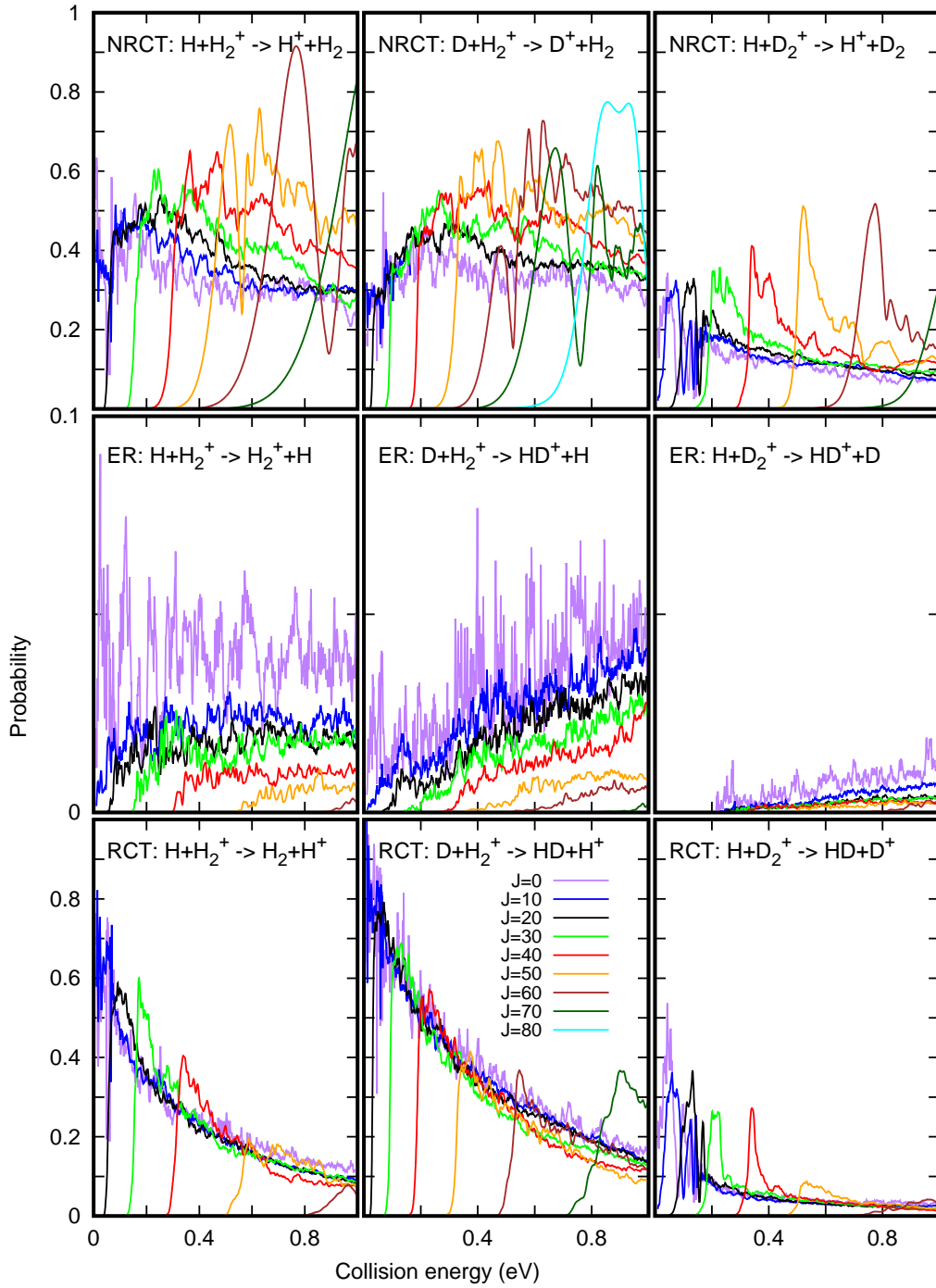


FIG. 4. Total reaction probability at different total angular momentum, J , for $\text{H}+\text{H}_2^+(v=0,j=0)$ (left panels), $\text{D}+\text{H}_2^+(v=0,j=0)$ (middle panels) and $\text{H}+\text{D}_2^+(v=0,j=0)$, towards the inelastic charge transfer, NRCT (H^++H_2 , D^++H_2 and H^++D_2 products in the top panels), the reactive channel, ER ($\text{H}+\text{H}_2^+$, $\text{H}+\text{HD}^+$ and $\text{D}+\text{HD}^+$ in the middle panels) and reactive charge transfer, RCT, channels (H^++H_2 , H^++HD and D^++HD in the bottom panels).

one. This explains why here the RCT is nearly identical to NRCT in this case.

The NRCT for the $\text{H}+\text{D}_2^+(v=0,j=0)$ reaction is compared with the experimental work of Andrianarijaona *et al.*^{66,67} in the top panel of Fig. 5. In these measurements of the $\text{H}+\text{D}_2^+$ reactions, only H^+ products are detected, so that their cross

section only corresponds to the NRCT process. The good agreement obtained with the present results, specially at energies of ≈ 0.6 eV, already demonstrates the adequacy of the simulations done here. It should be noted, however, that the D_2^+ reactants are produced with some vibrational excitation. This could explain why at lower energies the agreement is

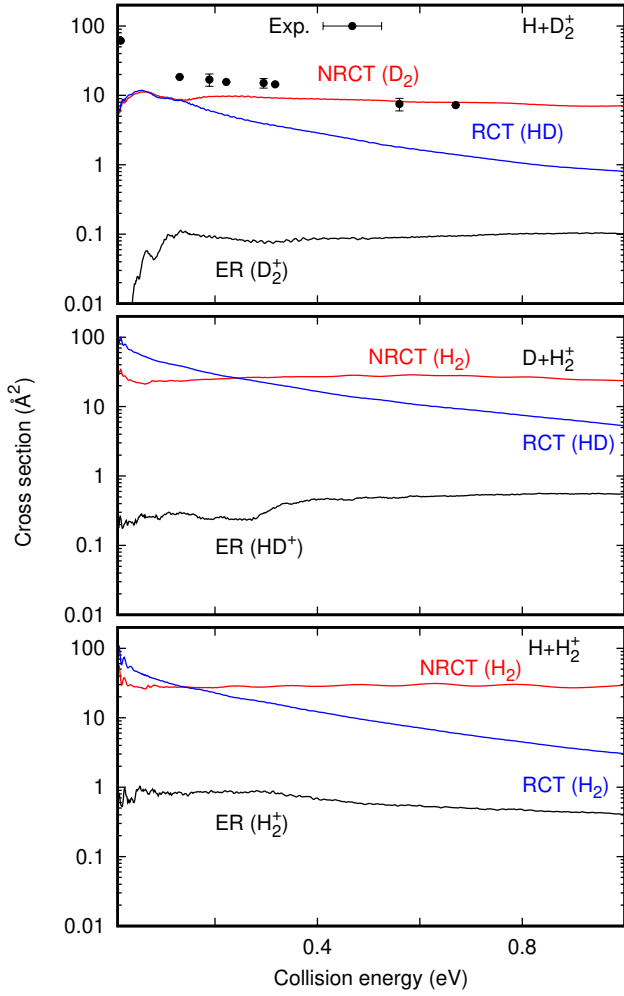


FIG. 5. Total integral reactive cross sections for $\text{H}+\text{H}_2^+(v=0,j=0)$ (bottom panel), $\text{D}+\text{H}_2^+(v=0,j=0)$ (middle panel) and $\text{H}+\text{D}_2^+(v=0,j=0)$ (top panel), towards the inelastic charge transfer, NRCT (H^++H_2 , D^++H_2 and H^++D_2 products), the reactive channel, ER ($\text{H}+\text{H}_2^+$, $\text{H}+\text{HD}^+$ and $\text{D}+\text{HD}^+$ products) and reactive charge transfer, RCT, channels (H^++H_2 , H^++HD and D^++HD). In the top panel the points correspond to the experimental values from Ref.^{66,67}

worse. Some studies on the vibrational effects are now under way.

The NRCT dominates the high energy region because the nearly resonant conditions between $\text{H}_2(v'=4)$ and the $\text{H}_2^+(v=0)$ levels (or $\text{D}_2^+(v=0)$ and $\text{D}_2(v'=6)$), as discussed for the reaction probabilities. The vibrationally resolved NRCT cross sections, in Fig. 6, also show this effect. In the first two reactions, below the $\text{H}_2(v'=4)$ channel opens, at 0.064 eV, $\text{H}_2(v')$ are formed progressively in ascending order, $v'=0,1,2$ and 3. There are small isotopic effects, but in general the NRCT shows a typical decreasing behaviour associated to exothermic reactions. At energies above 0.064 eV, $\text{H}_2(v'=4)$ opens, and the cross section for this channels increases becoming the dominant channel at energies above 0.2 eV. A similar situation holds for $\text{H}+\text{D}_2^+(v=0)$, but replacing $\text{H}_2(v'=4)$ by $\text{D}_2(v'=6)$.

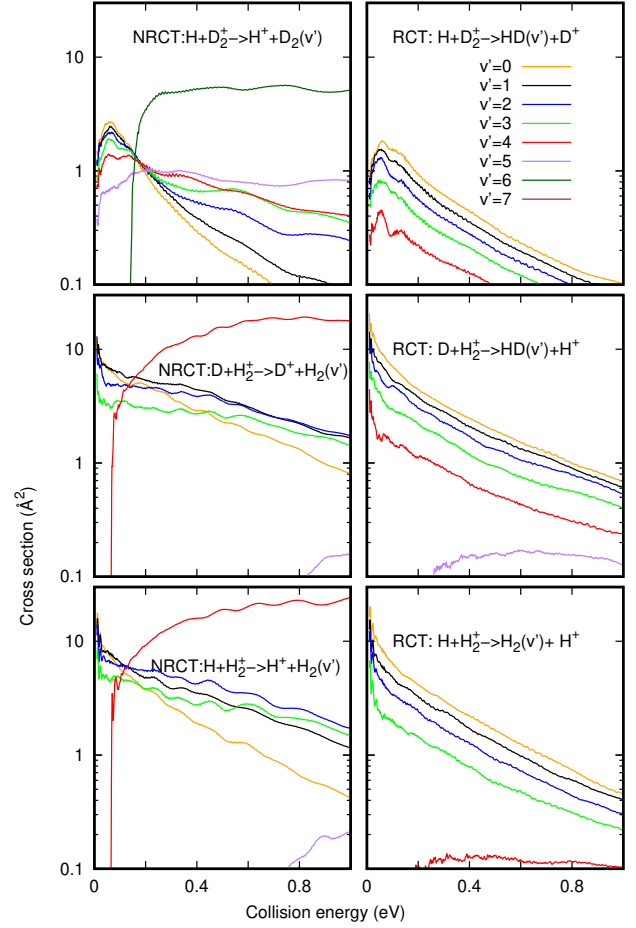


FIG. 6. Vibrationally resolved charge transfer cross sections for $\text{H}+\text{H}_2^+(v=0,j=0)\rightarrow\text{H}^++\text{H}_2(v')/\text{H}_2(v')+\text{H}^+$ (bottom panels) $\text{D}+\text{H}_2^+(v=0,j=0)\rightarrow\text{D}^++\text{H}_2(v')/\text{HD}(v')+\text{H}^+$ (middle panels) and $\text{H}+\text{D}_2^+(v=0,j=0)\rightarrow\text{H}^++\text{D}_2(v')/\text{HD}(v')+\text{D}^+$ (top panels), for the NRCT (left panels) and RCT (right panels) processes.

The vibrational resolved cross sections of Fig. 6 are in qualitative agreement with the results in Fig. 7 by Krstic⁷¹, which includes both NRCT and RCT processes calculated in a broader energy range using a close coupling method based on the infinite order sudden approximation (IOSA) with Delves hyperspherical coordinates. In Krstic work, $v'=4$ cross-section is always the most important, but it becomes of the same order than that for $v'=3$ at collision energies of 0.2 eV. Below 0.2 eV all $\sigma_{v=0\rightarrow v'}$ CT cross sections are of the order of 10 \AA^2 ²⁷¹, and for all $v'\neq 4$ decreases monotonically until 3 eV. At 1 eV the cross section for $v'=3$ is of the order of 1 \AA^2 , similar to the present results of NRCT+RCT. The differences arise about the position of the crossing between $v'=4$ and the other v' , and on the relative magnitude of the cross section associated to different v' 's. Since the method used here is more accurate, it may be concluded that at energies below 1 eV the present results are more accurate.

The calculations of Last *et al.*⁴⁸ were done from 0.06 to 0.21 eV using a quantum method based on negative imaginary

potential combined with a variational quantum method in a L^2 basis set. Their NRCT final vibrational distributions pick at $v'=3$, instead of 4. However, they used the helicity decoupling approximation, *i.e.* they did not consider the coupling between different helicities Ω . In this case, this approximation is not appropriate, because there are strong couplings between the different resonances with different Ω value originated by the deep well in the ground electronic state. However, the reason why their results are picked at $v'=3$ and not $v'=4$ should be related to the use of different potentials for the H_2 and H_2^+ fragments or to the extension of non-adiabatic couplings.

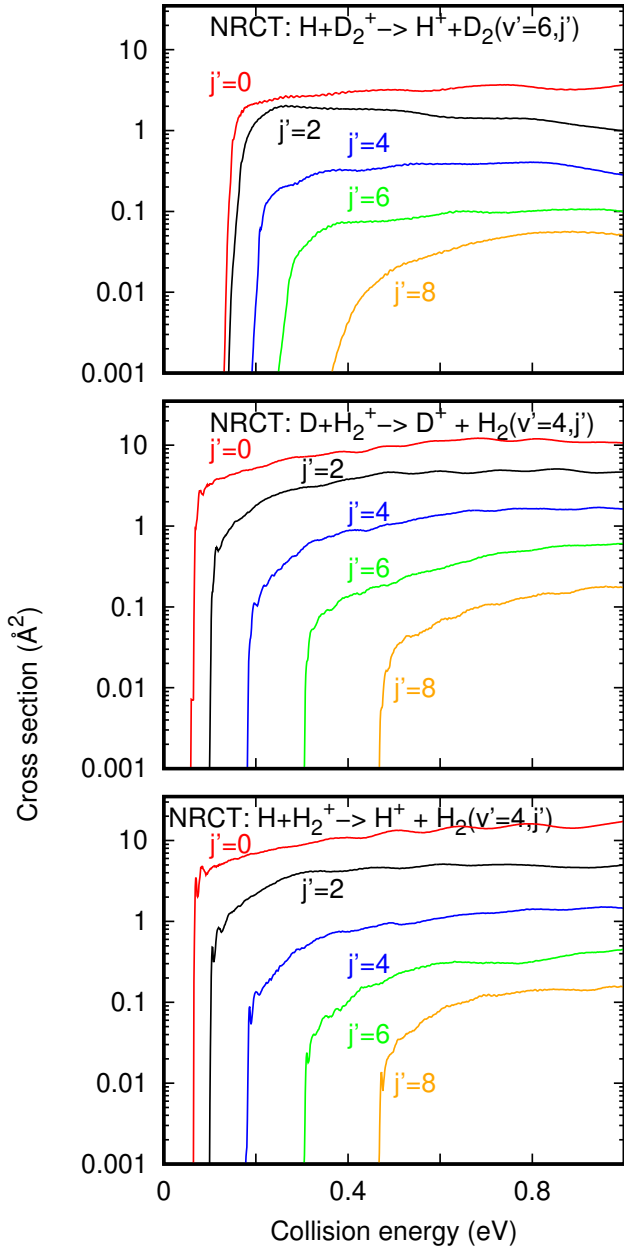


FIG. 7. Rotationally resolved NRCT cross sections for $H+H_2^+(v=0, j=0) \rightarrow H^+ + H_2(v'=4, j')$ (bottom panel), $D+H_2^+(v=0, j=0) \rightarrow D^+ + H_2(v'=4, j')$ (middle panel) and $H+D_2^+(v=0, j=0) \rightarrow H^+ + D_2(v'=6, j')$ (top panel).

The rotationally resolved NRCT cross sections for $H/D+H_2^+(v=0, j=0) \rightarrow H^+/D^+ + H_2(v'=4, j')$ and $H+D_2^+(v=0, j=0) \rightarrow H^+ + D_2(v'=6, j')$ collisions, in Fig. 7, clearly show that $j'=0$ is the dominant final rotational state, which is the closer to the $H_2^+(v=0, j=0)$ or $D_2^+(v=0, j=0)$ initial state. $j'=2/j'=0$ ratio is about a factor of 1/4 for collision energies above 0.3 eV, and this ratio decreases with rotational excitation of CT products. Last *et al.*⁴⁸ also reported the maximum of the state-to-state cross section for final $H_2(v'=4, j'=0)$ state, but less than a factor of 2 as compared to $v'=3, j'=4$.

Finally, it should be noted that while the results are accurate for $D+H_2^+$ and $H+D_2^+$, for $H+H_2^+$ we are including also the non-physical A_1 irreducible representation. While some work is now in progress to include the full permutation symmetry for $H+H_2^+$, we can already use as exact the para-to-ortho state-to-state cross sections. Moreover, because of the high propensity of the NRCT to final $H_2(v'=0, j'=0)$, some conclusions can be extracted. Thus, the present results for $H+H_2^+$ assess that the NRCT channel is dominant for energies above 0.2 eV up to 1 eV, in clear agreement with the results of Karpas *et al.*⁶⁴.

IV. CONCLUSIONS

In this work accurate quantum calculations have been presented for the $H/D+H_2^+$ and $H + D_2^+$ non-adiabatic charge transfer reactions using an accurate 3×3 diabatic potential matrix recently proposed⁷⁴, which includes long range interactions. It is found that the dominant channel corresponds to the resonant non-reactive charge transfer from $H_2^+(v=0)$ to $H_2(v'=4)$ and $D_2^+(v=0)$ to $D_2(v'=6)$, which is enhanced by their nearly resonant energies and the long-range dependence of the non-adiabatic couplings. This enhancement is based on rather general features of the H_3^+ asymptotic features, namely the electronic crossing and the energy difference of the vibrational states of the neutral and cation systems, and are not expected to depend on the accuracy of the PESs used in this work. The only requirement is to include the electronic coupling existing at rather long distances between the reactants, which is described very accurately by the PESs used in this work.

For $D+H_2^+$ and $H+D_2^+$ state-to-state cross sections are presented for the first time. For $H+H_2^+$ some caution must be paid because the permutation symmetry is not fully accounted, while some work is now-a-days in progress to include the permutation among the three fermions. In spite of that, the present results show a good qualitative agreement with the experimental data of Karpas *et al.*⁶⁴, who also reported that the CT channels dominate at ≈ 1.8 eV. The rather good agreement with the NRCT cross sections measured for $H+D_2^+$ by Andrianarijaona *et al.*^{66,67} already demonstrates the adequacy of the simulations presented here for $E > 0.5$ eV. However, a further study on the vibrational effect of the D_2^+ reactants should be done to understand the behavior at lower energies. It is also necessary to extend the present calculations to other rovibrational states and isotopic variants to provide reaction rate

constants of interest in astrophysical models of the Early Universe.

V. ACKNOWLEDGEMENTS

We acknowledge Dr. Andrianarijaona for providing us with the experimental data and very interesting discussions of their results. The research leading to these results has received fundings from MICIU (Spain) under grant FIS2017-83473-C2. We also acknowledge computing time at Finisterre (CESGA) and Marenstrum (BSC) under RES computational grants ACCT-2019-3-0004 and AECT-2020-1-0003, and CCC (UAM).

VI. DATA AVAILABILITY

The data that support the findings of this study are available from the corresponding author upon reasonable request.

REFERENCES

- ¹T. Oka, “Chemistry, astronomy and physics of H_3^+ ,” *Phil. Trans. R. Soc. A* **370**, 4991 (2012).
- ²T. Oka, “Interstellar H_3^+ ,” *Chem. Rev.* **113**, 8738 (2013).
- ³W. D. Watson, “The rate of formation of interstellar molecules by ion-molecule reactions,” *Astrophys. J.* **183**, L17 (1973).
- ⁴E. Herbst and W. Klemperer, “The formation and depletion of molecules in dense interstellar clouds,” *Astrophys. J.* **185**, 505 (1973).
- ⁵T. J. Millar, A. Bernett, and E. Herbst, “Deuterium fractionation in dense interstellar clouds,” *Astrophys. J.* **340**, 906 (1989).
- ⁶L. Pagani, M. Salez, and P. Wannier, “The chemistry of H_2D^+ in cold clouds,” *Astron. Astrophys.* **258**, 479 (1992).
- ⁷J. Tennyson, “Spectroscopy of H_3^+ : planets, chaos and the Universe,” *Rep. Prog. Phys.* **58**, 412 (1995).
- ⁸B. J. McCall and T. Oka, “ H_3^+ an ion with many talents (perspective),” *Science* **287**, 1941 (2000).
- ⁹S. C. Glover, “Comparing gas-phase and grain-catalyzed H_2 formation,” *Astrophys. J.* **584**, 331 (2003).
- ¹⁰V. Wakelam, E. Bron, S. Cazaux, F. Dulieu, C. Gry, P. Guillard, E. Habart, L. Hornekaer, S. Morisset, G. Nyman, V. Pirronello, S. D. Price, V. Valdivia, G. Vidali, and N. Watanabe, “ H_2 formation on interstellar dust grains: The viewpoints of theory, experiments, models and observations,” *Molecular Astrophysics* **9**, 1 – 36 (2017).
- ¹¹I. R. McNab, “The spectroscopy of H_3^+ ,” *Adv. Chem. Phys.* **89**, 1 (1995).
- ¹²E. Herbst, “The astrochemistry of H_3^+ ,” *Phil. Trans. R. Soc. Lond. A* **358**, 2523 (2000).
- ¹³D. Gerlich, P. Jusko, Š. Roučka, I. Zymak, R. Plašil, and J. Glosík, “Ion trap studies of $H^- + H \rightarrow H_2 + e^-$ between 10–135 K,” *Ap. J.* **749**, 22 (2012).
- ¹⁴Special issue, “Chemistry, astronomy and physics of H_3^+ ,” *Phil. Trans. R. Soc. A* **370** (2012).
- ¹⁵Special issue, “Advances in hydrogen molecular ions: H_3^+ , H_5^+ and beyond,” *Phil. Trans. R. Soc. A* **377** (2019).
- ¹⁶T. Oka, “Observation of the infrared spectrum of H_3^+ ,” *Phys. Rev. Lett.* **45**, 531 (1980).
- ¹⁷T. R. Geballe and T. Oka, “An infrared spectroscopic search for the molecular ion H_3^+ ,” *AstroPhys. J.* **342**, 855 (1989).
- ¹⁸T. R. Geballe, B. J. McCall, K. H. Hinkle, and T. Oka, “Detection of H_3^+ in the diffuse interstellar medium: the galactic and Cygnus OB2 number 12,” *AstroPhys. J.* **510**, 251 (1999).
- ¹⁹B. J. McCall, T. R. Geballe, K. H. Hinkle, and T. Oka, “Observations of H_3^+ in dense molecular Clouds,” *AstroPhys. J.* **522**, 338 (1999).
- ²⁰T. Oka, “Interstellar H_3^+ ,” *PNAS* **103**, 12235 (2006).
- ²¹O. L. Polyansky, A. Alijah, N. F. Zobov, I. I. Mizus, R. I. Ovsyannikov, J. Tennyson, L. Lodi, T. Szidarovszky, and A. G. Császár, “Spectroscopy of H_3^+ based on a new high-accuracy global potential energy surface,” *Philos Trans A Math Phys Eng Sci* **370**, 5014 (2012).
- ²²R. A. Bachorz, W. Cencek, R. Jaquet, and J. Komasa, “Rovibrational energy levels of H_3^+ with energies above the barrier to linearity,” *The Journal of chemical physics* **131**, 024105 (2009).
- ²³L. Velilla, B. Lepetit, A. Aguado, J. A. Beswick, and M. Paniagua, “The H_3^+ rovibrational spectrum revisited with a global electronic potential energy surface,” *J. Chem. Phys.* **129**, 084307 (2008).
- ²⁴J. Tennyson, O. L. Polyansky, N. F. Zobov, A. Alijah, and A. G. Császár, “High-accuracy calculations of the rotation-vibration spectrum of H_3^+ ,” *J. Phys. B: At. Mol. Opt. Phys.* **50**, 232001 (2017).
- ²⁵T. Furtenbacher, T. Szidarovsky, E. Matyus, C. Fabri, and A. G. Csaszar, “Analysis of the Rotational-Vibrational states of the molecular ion H_3^+ ,” *Journal of Chemical Theory and Computation* (2013).
- ²⁶R. Jaquet, W. Cencek, W. Kutzelnigg, and J. Rychlewski, “Sub-microhartree accuracy potential energy surface for H_3^+ including adiabatic and relativistic effects. II. Rovibrational analysis for H_3^+ and D_3^+ ,” *The Journal of Chemical Physics* **108**, 2837 (1998), <https://doi.org/10.1063/1.475703>.
- ²⁷J. Tennyson and O. L. Polyansky, “Non-Born-Oppenheimer correction to the H_3^+ potential from experimental data,” *Phys. Rev. A* **50**, 314 (1994).
- ²⁸J. Tennyson, B. M. Dinelli, and O. L. Polyansky, “On the determination of potential energy surfaces of spectroscopic accuracy,” *Journal of Molecular Structure: THEOCHEM* **341**, 133 (1995).
- ²⁹W. Cencek, J. Rychlewski, R. Jaquet, and W. Kutzelnigg, “Sub-microhartree accuracy potential energy surface for H_3^+ including adiabatic and relativistic effects. I. Calculation of the potential points,” *J. Chem. Phys.* **108**, 2831 (1998).
- ³⁰M. Pavanello, L. Adamowicz, A. Alijah, N. F. Zobov, I. I. Mizus, O. L. Polyansky, J. Tennyson, T. Szidarovszky, and A. G. Császár, “Calibration-quality adiabatic potential energy surfaces for H_3^+ and its isotopologues,” *J Chem Phys* **136**, 184303 (2012).

- ³¹I. I. Mizus, O. L. Polyansky, L. K. McKemmish, J. Tenynson, A. Alijah, and N. F. Zobov, "A global potential energy surface for H_3^+ ," *Molecular Physics* **117**, 1663 (2018).
- ³²L. Velilla, M. Paniagua, and A. Aguado, "Basis set convergence of potential energy surfaces: Ground electronic state of H_2 and H_3^+ ," *International Journal of Quantum Chemistry* **111**, 387 (2010).
- ³³R. Röhse, W. Kutzelnigg, R. Jaquet, and W. Klopper, "Potential energy surface of the H_3^+ ground state in the neighborhood of the minimum with microhartree accuracy and vibrational frequencies derived from it," *The Journal of chemical physics* **101**, 2231–2243 (1994).
- ³⁴L. P. Viegas, A. Alijah, and A. J. C. Varandas, "Accurate ab initio based multisheeted double many-body expansion potential energy surface for the three lowest electronic singlet states of H_3^+ ," *J Chem Phys* **126**, 074309 (2007).
- ³⁵S. Ghosh, S. Mukherjee, B. Mukherjee, S. Mandal, R. Sharma, Pinaki Chaudhury, and S. Adhikari, "Beyond Born-Oppenheimer theory for ab initio constructed diabatic potential energy surfaces of singlet H_3^+ to study reaction dynamics using coupled 3D time-dependent wave-packet approach," *J. Chem. Phys.* **147**, 074105 (2017).
- ³⁶C. Schlier, U. Novotny, and E. Teloy, "Proton-hydrogen collisions," *Chem. Phys.* **111**, 401 (1987).
- ³⁷D. Gerlich, "Ortho-para transitions in reactive $H^+ + H_2$ collisions," *J. Chem. Phys.* **92**, 2377 (1990).
- ³⁸D. Gerlich, "Inhomogeneous RF fields: a versatile tool for the study of processes with slow ions," *Adv. Chem. Phys.* **82**, 1 (1992).
- ³⁹D. Gerlich and S. Schlemmer, "Deuterium fractionation in gas-phase reactions measured in the laboratory," *Planet. Space Sci.* **50**, 1287 (2002).
- ⁴⁰D. W. Savin, P. S. Krstic, Z. Haiman, and P. C. Stancil, "Rate coefficient for $H^+ + H_2(X, v=0, j=0) \rightarrow H(1s) + H_2^+$ charge transfer and some cosmological implications," *Astro-Phys. J.* **606**, L170 (2004).
- ⁴¹T. Kusakabe, L. Pichl, R. J. Buenker, M. Kimura, and H. Tawara, "Isotope effect in charge-transfer collisions of slow H^+ and D^+ ions with H_2 , HD and D_2 molecules," *Phys. Rev. A* **70**, 052710 (2004).
- ⁴²D. Dai, C. C. Wang, G. Wu, S. A. Harich, H. Song, M. Hayes, D. G. R. T. Skodje, and X. Yang, "State-to-state dynamics of high- n Rydberg H-atom scattering with D_2 ," *Phys. Rev. Lett.* **95**, 013201 (2005).
- ⁴³E. Carmona-Novillo, T. González-Lezana, O. Roncero, P. Honvault, J. M. Launay, N. Bulut, F. J. Aoiz, L. Bañares, A. Trottier, and E. Wrede, "On the dynamics of the $H^+ + D_2(v=0, j=0) \rightarrow HD + D^+$ reaction: a comparison between theory and experiment," *J. Chem. Phys.* **128**, 014304 (2008).
- ⁴⁴H. Song, D. Dai, G. Wu, C. C. Wang, S. A. Harich, M. Hayes, X. Y. X. Wang, D. Gerlich, and R. T. Skodje, "Chemical reaction dynamics of Rydberg atoms with neutral molecules: A comparison of molecular-beam and classical trajectory trajectory results for the $H(n) + D_2 \rightarrow HD + D(n')$ reaction," *J. Chem. Phys.* **123**, 074314 (2005).
- ⁴⁵X. Urbain, N. de Ruette, V. M. Andrianarijaona, M. F. Martin, L. F. Menchero, L. Errea, L. Méndez, I. Rabadan, and B. Pons, "iNew light shed on charge transfer in fundamental $H^+ + H_2$," *Phys. Rev. Lett.* **111**, 203201 (2013).
- ⁴⁶N. Markovic and G. D. Billing, *Chem. Phys.* **191**, 247 (1995).
- ⁴⁷A. Ichihara, T. Shirai, and K. Yokoyama, *J. Chem. Phys.* **105**, 1857 (1996).
- ⁴⁸I. Last, M. Gilibert, and M. Baer, "A three-dimensional quantum mechanical study of the $H + H_2^+ \rightarrow H_2 + H^+$ system: competition between chemical exchange and inelastic processes," *J. Chem. Phys.* **107**, 1451 (1997).
- ⁴⁹M. Chajia and R. D. Levine, "Reactive and nonreactive charge transfer by the FMS method: low energy $H^+ + D_2$ and $H + H_2^+$ collisions," *Phys. Chem. Chem. Phys.* **1**, 1205 (1999).
- ⁵⁰T. Takayanagi, Y. Kurosaki, and A. Ichihara, "Three-dimensional quantum reactive scattering calculations for the nonadiabatic $(D + H_2)^+$ reaction system," *J. Chem. Phys.* **112**, 2615 (2000).
- ⁵¹V. G. Ushakov, K. Nobusada, and V. Osherov, "Electronically nonadiabatic transitions in a collinear $H_2 + H^+$ system: Quantum mechanical understanding and comparison with a trajectory surface hopping method," *Phys. Chem. Chem. Phys.* **3**, 63 (2001).
- ⁵²A. Ichihara, O. Iwamoto, and R. K. Janev, "Cross sections for the $H^+ + H_2(v=0-14) \rightarrow H + H_2^+$ at low collision energies," *J. Phys. B: At. Mol. Opt. Phys.* **33**, 4747 (2000).
- ⁵³L. F. Errea, A. Macías, L. Méndez, I. Rabadán, and A. Riera, "Limit of the vibrational sudden approximation for $H^+ + H_2$ collisions," *Phys. Rev. A* **65**, 010701 (2001).
- ⁵⁴H. Kamisaka, W. Bian, K. Nobusada, and H. Nakamura, "Accurate quantum dynamics of electronically nonadiabatic chemical reactions in the DH_2^+ system," *J. Chem. Phys.* **116**, 654 (2002).
- ⁵⁵P. S. Krstic and R. K. Janev, "Inelastic processes from vibrationally excited states in slow $H^+ + H_2$ and $H + H_2^+$ collisions. II. Dissociation," *Phys. Rev. A* **67**, 022708 (2003).
- ⁵⁶T.-S. Chu and K.-L. Han, "Nonadiabatic time-dependent wave packet study of the $D^+ + H_2$ reaction system," *J. Phys. Chem. A* **109**, 2050 (2005).
- ⁵⁷T. González-Lezana, A. Aguado, M. Paniagua, and O. Roncero, "Quantum approaches for the insertion dynamics of the $H^+ + D_2$ and $D^+ + H_2$ reactive collisions," *J. Chem. Phys.* **123**, 194309 (2005).
- ⁵⁸T. González-Lezana, O. Roncero, P. Honvault, J. M. Launay, N. Bulut, F. J. Aoiz, and L. Bañares, "A detailed quantum mechanical and quasiclassical trajectory study on the dynamics of the $H^+ + H_2 \rightarrow H_2 + H^+$ exchange reaction," *J. Chem. Phys.* **125**, 094314 (2006).
- ⁵⁹T. González-Lezana and P. Honvault, "The $H^+ + H_2$ reaction," *Int. Rev. Phys. Chem* **33**, 371 (2014).
- ⁶⁰T. González-Lezana and P. Honvault, "Rovibrational transitions of H_2 by collision with H^+ at high temperature," *Monthly Not. Roy. Astron. Soc.* **467**, 1294 (2017).
- ⁶¹T. Sahoo, S. Ghosh, S. Adhikari, R. Sharma, and A. J. C. Varandas, "Coupled 3D Time-Dependent Wave-Packet Approach in Hyperspherical Coordinates: Application to the Adiabatic Singlet-State($1^1A'$) $D^+ + H_2$ Reaction," *J. Phys. Chem. A* **118**, 4837 (2014).

- ⁶²S. Ghosh, T. Sahoo, S. Adhikari, R. Sharma, and A. J. C. Varandas, "Coupled 3D Time-Dependent Wave-Packet Approach in Hyperspherical Coordinates: The $D^+ + H_2$ Reaction on the Triple-Sheeted DMBE Potential Energy Surface," *J. Phys. Chem. A* **119**, 12392 (2015).
- ⁶³X. Urbain, A. Dochain, R. Marion, T. Launoy, and J. Loreau, "Photodissociation as a probe of the H_3^+ avoided crossing seam," *Phil. Trans. R. Soc. A* **377**, 20180399 (2019).
- ⁶⁴Z. Karpas, V. Anicich, and W. T. Huntress, "An ion cyclotron resonance study of reactions of ions with hydrogen atoms," *J. Chem. Phys.* **70**, 2877 (1979).
- ⁶⁵P. C. E. McCartney, C. McGrath, J. W. McConkey, M. B. Shah, and J. Geddes, "Collisions of H_2^+ with H: individual fragmentation channels," *J. Phys. B: At. Mol. Opt. Phys.* **32**, 5103 (1999).
- ⁶⁶V. M. Andrianarijaona, J. J. Rada, R. Rejoub, and C. C. Havener, "Investigation of charge transfer in low energy $D_2^+ + H$ collisions using merged beams," *J. Phys.: Conf. Ser.* **194**, 012043 (2009).
- ⁶⁷V. M. Andrianarijaona and L. M. Wegley and A. Z. Watson and M. Andrianarijaona and C. P. DeGuzman and K. Kim and E. J. Nuss and J. J. Taylor and R. L. Wilson and R. T. Zhang and D. G. Seely and C. C. Havener, "Absolute measurement of the total cross section in 2 keV/u - 10 keV/u $D_2^+ + H$ charge transfer collisions," *AIP Conference Proceedings* **2160**, 070005 (2019).
- ⁶⁸C. M. Coppola, S. Longo, M. Capitelli, F. Palla, and D. Galli, "Vibrational level population of H_2 and H_2^+ in the early universe," *The Astrophysical Journal Supplement Series* **193**, 7 (2011).
- ⁶⁹N. Indriolo and B. J. McCall, "Investigating the cosmic-ray ionization rate in galactic diffuse interstellar medium through observations of H_3^+ ," *AstroPhys. J.* **745**, 91 (2012).
- ⁷⁰C. M. Coppola, D. Galli, F. Palla, S. Longo, and J. Chluba, "Non-thermal photons and H_2 formation in the early Universe," *Monthly Notices of the Royal Astronomical Society* **434**, 114 (2013).
- ⁷¹P. S. Krstić, "Inelastic processes from vibrationally excited states in slow $H^+ + H_2$ and $H + H_2^+$ collisions: Excitations and charge transfer," *Phys. Rev. A* **66**, 042717 (2002).
- ⁷²L. F. Errea, A. Macias, L. Méndez, I. Rabadán, and A. Riera, "Charge transfer in $H_2^+ - H(1s)$ collisions," *Nuclear Instruments and Methods Phys. Research B* **235**, 362 (2005).
- ⁷³S. Ghosh, T. Sahoo, M. Baer, and S. Adhikari, "Charge transfer processes for $H + H_2^+$ reaction employing coupled 3D wavepacket approach on beyond Born-Oppenheimer based ab initio constructed diabatic potential energy surfaces," *J. Phys. Chem. A* **ASAP on-line**, doi:10.1021/acs.jpca.0c08975 (2021).
- ⁷⁴A. Aguado, O. Roncero, and C. Sanz-Sanz, "Three states global fittings with improved long range: singlet and triplet states of H_3^+ ," *PCCP* doi: **10.1039/D0CP04100A** (2021).
- ⁷⁵J. C. Tully, "Semiempirical Diatomics-in-Molecules potential Energy surfaces," *Adv. Chem. Phys.* **42**, 63 (1980).
- ⁷⁶H.-J. Werner, P. J. Knowles, G. Knizia, F. R. Manby, and M. Schütz, "Molpro: a general-purpose quantum chemistry program package," *WIREs Comput Mol Sci* **2**, 242–253 (2012).
- ⁷⁷T. H. Dunning and Jr., "Dunning electronic basis set functions -1," *J. Chem. Phys.* **90**, 1007 (1989).
- ⁷⁸M. Baer, "Adiabatic and diabatic representations for atom-molecule collisions: treatment of the collinear arrangement," *Chem. Phys. Lett.* **35**, 112 (1975).
- ⁷⁹C. A. Mead and D. G. Truhlar, "Conditions for the definition of a strictly diabatic electronic basis for molecular systems," *J. Chem. Phys.* **77**, 6090 (1982).
- ⁸⁰A. Thiel and H. Köppel, "Proposal and numerical test of a simple diabaticization scheme," *J. Chem. Phys.* **110**, 9371 (1999).
- ⁸¹S. Gómez-Carrasco, A. Aguado, M. Paniagua, and O. Roncero, "Coupled diabatic potential energy surfaces for studying the non-adiabatic dynamics at conical intersections in angular resolved photodetachment simulations of $OHF^- \rightarrow OHF + e^-$," *J. Chem. Phys.* **125**, 164321 (2006).
- ⁸²H. Köppel, "Diabatic representation: methods for the construction of diabatic electronic states," in *Conical Intersections: electronic structure, dynamics and spectroscopy*, edited by D. Y. W. Domcke and H. Köppel (Advanced series in Physical Chemistry, World Scientific Publishing Co., 2004) p. 175.
- ⁸³A. Aguado, M. Paniagua, M. Lara, and O. Roncero, "Potential energy surface and wave packet calculations on the $Li + HF \rightarrow LiF + H$ reaction," *J. Chem. Phys.* **106**, 1013 (1997).
- ⁸⁴M. Paniagua, A. Aguado, M. Lara, and O. Roncero, "Transition state spectroscopy on the $LiHF$ system," *J. Chem. Phys.* **109**, 2971 (1998).
- ⁸⁵A. Aguado, M. Paniagua, C. Sanz-Sanz, and O. Roncero, "Transition state spectroscopy of the excited electronic states of $Li-HF$," *J. Chem. Phys.* **119**, 10088 (2003).
- ⁸⁶A. Zanchet, O. Roncero, T. González-Lezana, A. Rodríguez-López, A. Aguado, C. Sanz-Sanz, and S. Gómez-Carrasco, "Differential cross sections and product rotational polarization in a+bc reactions using wave packet methods: $H^+ + D_2$ and $Li + HF$ examples," *J. Phys. Chem. A* **113**, 14488 (2009).
- ⁸⁷S. Gómez-Carrasco and O. Roncero, "Coordinate transformation methods to calculate state-to-state reaction probabilities with wave packet treatments," *J. Chem. Phys.* **125**, 054102 (2006).
- ⁸⁸V. A. Mandelshtam and H. S. Taylor, "Spectral projection approach to quantum scattering calculations," *J. Chem. Phys.* **102**, 7390 (1995).
- ⁸⁹G. J. Kroes and D. Neuhauser, "Performance of a time-independent scattering wave packet technique using real operators and wave functions," *J. Chem. Phys.* **105**, 8690 (1996).
- ⁹⁰R. Chen and H. Guo, "Evolution of quantum system in order domain of chebyshev operator," *J. Chem. Phys.* **105**, 3569 (1996).
- ⁹¹S. K. Gray and G. G. Balint-Kurti, "Quantum dynamics with real wavepackets, including application to three-dimensional ($j=0$) $d + h_2 \rightarrow hd + h$ reactive scattering," *J. Chem. Phys.* **108**, 950 (1998).

- ⁹²B. Lepetit and D. Lemoine, "State-to-state arhbr photodissociation quantum dynamics," *J. Chem. Phys.* **117**, 8676 (2002).
- ⁹³O. Roncero, D. Caloto, K. C. Janda, and N. Halberstadt, "From the sparse to the statistical limit of intramolecular vibrational redistribution in vibrational predissociation: ArCl₂ as an example," *J. Chem. Phys.* **107**, 1406 (1997).
- ⁹⁴A. Zanchet, B. Godard, N. Bulut, O. Roncero, P. Halvick, and J. Cernicharo, "H₂(*v*=0,1)+C(²P) → H+CH⁺ state-to-state rate constants for chemical pumping models in astrophysical media," *ApJ* **766**, 80 (2013).
- ⁹⁵J. M. Bowman, "Reduced dimensionality theories of quantum reactive scattering," *Adv. Chem. Phys.* **61**, 115 (1985).
- ⁹⁶C. Sanz, O. Roncero, C. Tablero, A. Aguado, and M. Paniagua, "The lowest triplet ³A' of H₃⁺: Global potential energy surface and vibrational calculations," *J. Chem. Phys.* **114**, 2182 (2001).
- ⁹⁷W. H. Miller, "Coupled equations and the minimum principle for collisions of an atom and a diatomicmolecule, including rearrangements," *J. Chem. Phys.* **50**, 407 (1969).
- ⁹⁸P. Honvault, M. Jorfi, T. González-Lezana, A. Faure, and L. Pagani, "Ortho-para conversion by proton exchange at low temperature: an accurate quantum mechanical study," *Phys. Rev. Lett.* **107**, 023201 (2011).